Journal of Nanobiotechnology

RESEARCH Open Access

Nanosilicates facilitate periodontal regeneration potential by activating the PI3K-AKT signaling pathway in periodontal ligament cells

Ziqin Chen[1,2], Nianqi Xiao[3], Lan Luo[1,2], Lu Zhang[1,2], Fan Yin[1,2], Weiqiang Hu[1,2], Zekai Wu[1,2], Yuling Chen[1,2], Kai Luo[1,2*] and Xiongcheng Xu[1,2*]

Abstract

The recent development of nanobiomaterials has shed some light on the field of periodontal tissue regeneration. Laponite (LAP), an artificially synthesized two-dimensional (2D) disk-shaped nanosilicate, has garnered substantial attention in regenerative biomedical applications owing to its distinctive structure, exceptional biocompatibility and bioactivity. This study endeavors to comprehensively evaluate the influence of LAP on periodontal regeneration. The effects of LAP on periodontal ligament cells (PDLCs) on osteogenesis, cementogenesis and angiogenesis were systematically assessed, and the potential mechanism was explored through RNA sequencing. The results indicated that LAP improved osteogenic and cementogenic differentiation of PDLCs, the regulatory effects of LAP on PDLCs were closely correlated with activation of PI3K-AKT signaling pathway. Moreover, LAP enhanced angiogenesis indirectly *via* manipulating paracrine of PDLCs. Then, LAP was implanted into rat periodontal defect to confirm its regenerative potential. Both micro-CT and histological analysis indicated that LAP could facilitate periodontal tissue regeneration in vivo. These findings provide insights into the bioactivity and underlying mechanism of LAP on PDLCs, highlighting it might be a potential therapeutic option in periodontal therapy.

Keywords Nanosilicate, Periodontal ligament cells, PI3K-AKT pathway, Periodontal regeneration

Introduction

Periodontitis disrupts periodontal supporting structures, including cementum, alveolar bone, and periodontal ligament, potentially leading to tooth loss [1, 2]. The ultimate goal of current periodontal therapy is to anatomically and functionally restore lost periodontal tissues [3, 4]. Some clinical periodontal regenerative techniques, including guided tissue regeneration (GTR) combined with bone grafting and growth factors, have been established to restore the damaged periodontal supporting structures [5, 6]. However, these techniques tremendously rely on the patient's own regenerative capacity, and their

*Correspondence:
Kai Luo
luokai39@163.com
Xiongcheng Xu
xiongchengxu@fjmu.edu.cn
[1]Fujian Key Laboratory of Oral Diseases & Fujian Provincial Engineering Research Center of Oral Biomaterial & Stomatological Key Laboratory of Fujian College and University, School and Hospital of Stomatology, Fujian Medical University, Fuzhou, P.R. China
[2]Institute of Stomatology & Laboratory of Oral Tissue Engineering, School and Hospital of Stomatology, Fujian Medical University, Fuzhou 350002, P.R. China
[3]Gannan Health Vocational College, Ganzhou, Jiangxi 341000, P.R. China

therapeutic efficacy are changeable and unpredictable [7–9].

The emergence of nanobiomaterials has made periodontal tissue regeneration a domain with breakthrough potential [10, 11]. 2D nanomaterials such as graphene and MXene had been reported to regulate osteogenic differentiation of PDLCs and accelerate periodontal regeneration [12, 13]. Laponite (LAP) is a two-dimensional (2D) nanosilicate with a diameter of less than 50 nm and a thickness of 1–2 nm created synthetically [14, 15]. LAP has been widely utilized in regenerative biomedical applications due to its unique characteristics, superior biocompatibility and biological activity [16]. Several studies indicated that LAP demonstrated superior cytocompatibility and could stimulate osteogenic differentiation of rat bone marrow mesenchymal stem cells (BMSCs), human mesenchymal stem cells (MSCs), human dental follicle stem cells (DFSCs) and human adipose derived stem cells (ADSCs) [17–20]. Our previous research has demonstrated that LAP can biofunctionally modify biomaterials [21, 22]. LAP-embedded polycaprolactone (PCL) improved the mechanical characteristics and facilitated rat BMSCs and osteoblasts to directly stimulate osteogenesis and indirectly control osteoclastogenesis and angiogenesis, eventually promoting bone formation in vivo [22]. It indicated that LAP had great potential in manipulating periodontal regeneration.

Periodontal ligament cells (PDLCs), with stem-cell-like properties, are extracted from the periodontal ligament and are considered the most promising seed cells for periodontal regeneration [23]. PDLCs can differentiate into osteoblasts and cementoblasts, regulate vascular endothelial cells to promote the formation of blood vessels, ultimately facilitating the regeneration of periodontal tissue [23–26]. However, the biological effect and particular mechanisms of LAP on PDLCs and periodontal regeneration is currently unclear. Therefore, the present study aimed to explore the intrinsic regulatory role of LAP on PDLCs and its effect on periodontal tissue regeneration. LAP was firstly co-cultured with PDLCs to evaluate its effects on osteogenesis, cementogenesis and angiogenesis, which exerted substantial effects for periodontal regeneration process. Then we evaluated the processes by which LAP acts on PDLCs and its regulatory effects on intracellular cascade reactions. Subsequently, LAP was implanted into rat experimental periodontal defect. Both microcomputed tomography (micro-CT) and histological assessment were performed to evaluate its effect on periodontal regeneration. This investigation will provide novel insights into the potential application of LAP in periodontal therapy.

Experimental section

Preparation of materials

LAPONITE-XLG (Nanocor Inc, China) was dissolved in 2 mL sterile water, shocked and ultrasonic stirring until complete dissolution to prepare an initial liquid with a concentration of 5 $mg{\cdot}mL^{-1}$.

Cell culture and identification

All experiments were approved by the Ethics of the School and Hospital of Stomatology, Fujian Medical University (2021 Ethics Review No. 104). PDLCs were isolated and cultured from mirror 1/3 of the human teeth root as previously described and cultured in α-MEM with 10% FBS [13]. The α-MEM medium was changed to osteogenic induction solutions (Cyagen, China), adipogenic induction medium (Cyagen, China), and chondroblast induction (Cyagen, China) to confirm the ability of differentiation. Mineralized nodules, lipogenic nodules and blue chondroblast cells were stained with Alizarin Red S, oil red O and Alysin blue respectively (Sigma Aldrich, USA). The stained cells were imaged using fluorescence microscopy (Zeiss, Germany). The surface markers of PDLCs were analyzed by flow cytometry. PDLCs were digested with 0.25% trypsin and collected suspension to incubate with FITC-labeled CD34, FITC-labeled CD45, FITC-labeled CD73 and FITC-labeled CD90, respectively, then analyzed by flow cytometer (BD Biosciences, USA).

Cell counting kit-8 (CCK-8) assay

A CCK-8 assay (Dojindo, Japan) was performed to measure cell proliferation at 1, 3, 5 and 7 days following the instructions. Cell viability at each time point was determined by measuring the optical density (OD) value at 450 nm using an iMark microplate reader (iMark, Bio-Rad Laboratories, USA).

Alkaline phosphatase (ALP) staining and mineral nodule formation assays

BCIP/NBT alkaline phosphatase kit (Beyotime, China) and ALP assay kit (Jiancheng Inc, China) were used to evaluate ALP staining and activity following osteogenic induction for 7 days. Alizarin Red S (pH 4.2) (Sigma, USA) and 10% cetylpyridinium chloride in 10 mM sodium phosphate (pH 7.0) were applied to observe and eluted the mineral nodule following osteogenic induction for 21 days.

Quantitative real-time polymerase chain reaction (PCR) analysis

A universal RNA extraction kit, PrimeScript RT Master Mix, and TB Green Premix ExTaq II (Takara, Japan) were used to extract total RNA from each sample, synthesize cDNA and perform qPCR respectively (Takara, Japan).

The primers were displayed in Table S1 (Supporting Information) and created by Sangon Biotech (Shanghai, China).

Western blot

Collecting the protein of cells stimulated with different concentrations of LAP for 7 days by using RIPA lysis buffer, proteins were separated by protein gel electrophoresis, and then transferred to polyvinylidene difluoride (PVDF) membranes. After 3 h closure using 5% skim milk powder, PVDF membranes were incubated with the primary antibodies ALPL (1:1000), COL1A1 (1:1000), RUNX2 (1:500), CAP (1:5000), CEMP1 (1:1000), P-AKT(1:1000), AKT(1:1000), PI3K(1:1000), P-mTOR (1:1000), mTOR (1:1000), GAPDH (1:1000) and Actin (1:5000). Then, using a secondary antibody (1:20000) to incubate the membranes. Enhanced chemiluminescence reagents were used to measure the levels of protein expression, and ImageJ was used to evaluate the results.

Intracellular uptake activity of LAP

PDLCs treated by 100 $\mu g \cdot mL^{-1}$ rhodamine-marked LAP were fixed, permeated, and blocked. Then, F-actin staining (FITC-phalloidin) and DAPI solution (Beyotime, China) were incubated in the cells gradually. Confocal laser scanning microscopy was used to visualize the labeled cells.

HUVECs cultured with conditioned medium of PDLCs

PDLCs were cultured by 0 $\mu g \cdot mL^{-1}$ and 100 $\mu g \cdot mL^{-1}$ LAP for 3 days with 1 mL medium. The supernatants of PDLCs without LAP were used as controls (0 $\mu g \cdot mL^{-1}$ group). Human umbilical vein endothelial cells (HUVECs) were obtained from the Cell Bank of the Chinese Academy of Sciences and grown in DMEM with 10% FBS supplemented with the acquired supernatants at a 1:1 ratio. Six-well plates containing HUVECs were scratched using a pipette tip. After that, supernatants were added in the manner previously stated. At each instant, the pictures were taken respectively. The wound regions were approximated by using Image J software. Matrigel matrix (Corning, USA) was put in the bottom of a 96-well plate. Then, HUVECs were cultured on the surface of the fixed matrix with different supernatants. The lengths of the tube-like structures were calculated by Image J software. Gene and protein expression levels of HUVECs were evaluated by qPCR and WB as described before on Day 3.

RNA sequencing and bioinformatics analysis

Transcriptome sequencing was performed to explore the mechanism of osteogenesis and cementogenic promotion by LAP. Total RNA was isolated from PDLCs stimulated by LAP using Trizol reagent (Takara, Japan) after 7 Days of cultivation, according to the manufacturer's instructions. Cells without LAP were used as the controls. RNA sequencing was performed at Wekemo Bioincloud to determine the expression profiles of the mRNAs in the groups of 0 $\mu g \cdot mL^{-1}$ and 100 $\mu g \cdot mL^{-1}$ LAP. mRNAs with a fold change of $\log_2 > 1$ or < -1 and $p < 0.05$ were considered differentially expressed. Gene ontology (GO) analysis was used for functional annotation of genes. Kyoto Encyclopedia of Genes and Genomes (KEGG) was used to analyze the signaling pathways in which differentially expressed genes were enriched. Bioinformatic analyses were performed using online Wekemo Bioincloud tools (https://bioincloud.tech/pipelines).

Inhibition of Pi3K-AKT signaling pathway

LY294002 (LY, MCE, USA) was dissolved in dimethyl sulfoxide (DMSO, MCE, USA) to prepare an initial liquid with a concentration of 5 mM. LY was diluted with medium to 10 μM, while the control and LAP group was added with the same amount of DMSO. The cells were randomly split into three groups: the Control+DMSO group, the LAP+DMSO group, and the LAP+LY group. After 6 h, the protein of cells was collected, and Western blot was performed as described in Section "Western blot". ALP staining and mineral nodule formation assays were performed as described in Section "Alkaline phosphatase (ALP) staining and mineral nodule formation assays". qPCR was performed as described in Section "Quantitative real-time polymerase chain reaction (PCR) analysis".

Rat periodontal defect surgical procedure

The study protocol was approved by the Animal Care and Use Committee of Fujian Medical University (IACUC FJMU 2023-0036). All rats were anesthetized via intraperitoneal injection of 40 mg/kg ketamine. The periodontal defect model was prepared in 4-week-old rat mandibles as our previously described [27]. A round bur was used to prepare periodontal defects with 2 mm height × 3 mm width × 1 mm depth around the first molar. The periodontal ligament was removed to expose the root surface. 10 rats were randomly split into two groups: the Control group with Collagen Sponge (CS, kejibang, China), the LAP group with LAP infiltrated in CS. 5 rats were included in each group. 24 Days later, all rats were sacrificed to collect mandibles.

Microcomputed tomography (micro-CT) analysis

The fixed mandibles samples were scanned by a micro-CT scanner (SCANCO μCT50, Switzerland). Three-dimensional images were obtained and analyzed using Mimics software (Mimics 20.0, Materialise, Leuven, Belgium). Cross-sections of micro-CT reconstructed images were near apical third area. Bone volume per total

volume ratio (BV/TV), bone mineral density (BMD) and trabecular number (Tb.N) were evaluated.

Histologic staining and analysis

The mandibles were decalcified in 10% ethylenediaminetetraacetic acid (EDTA), dehydrated and embedded. Consecutive sections were obtained from the defect area and stained using H&E and Masson's trichrome staining. For the periodontal defect model, the sections were near apical third area. The new bone areas and new attachment formation rate were assessed using ImageJ software.

Immunofluorescence staining and analysis

Consecutive sections were obtained from the defect area and immersed in antigen retrieval solution. Then, sections blocked with goat serum and incubated with primary antibodies against rat CD31 (1:100; ABclonal, China) as a vascular endothelial cell surface marker. Alexa Fluor 488-conjugated secondary antibody (1:500; Beyotime, China) was incubated for 1 h. Nuclei were stained with DAPI. The CD31-positive stained area was assessed using Image J software.

Statistical analysis

The mean and standard deviation are used to present data. To assess the variations across groups, the t test or one-factor analysis of variance was performed, followed by the Tukey's HSD post hoc test. $p<0.05$ was considered significant for all tests.

Results

LAP promoted osteogenic differentiation of PDLCs

PDLCs were successfully isolated and cultured from human extracted tooth. The multipotent differentiation capacities of PDLCs were confirmed after osteogenic, adipogenic and chondrogenic differentiation induction. Flow cytometry analysis indicated that PDLCs were negative for hematopoietic cell marker CD34 and CD45 (Fig. 1c-d), and were positive for mesenchymal stem cell

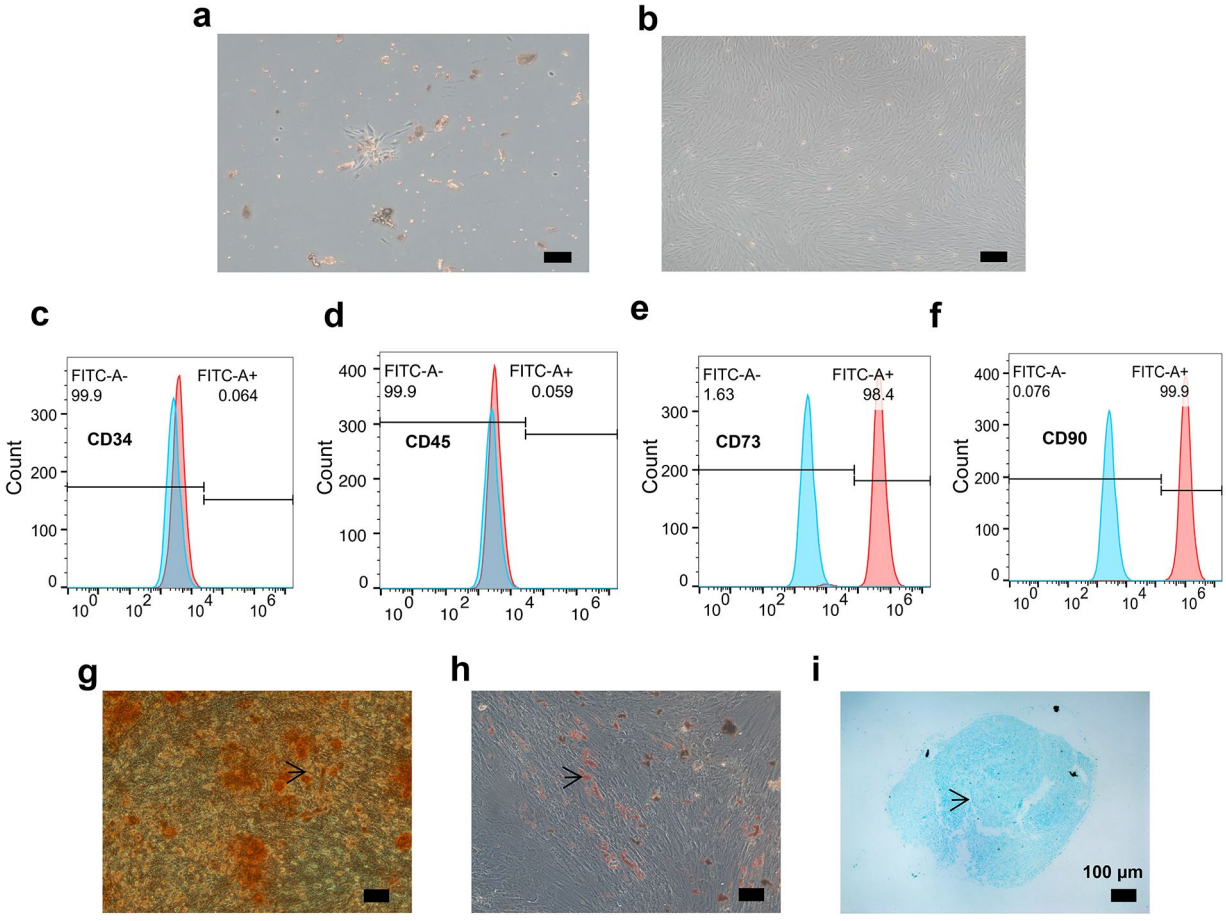

Fig. 1 Isolated and identification of PDLCs. (**a**-**b**) PDLCs cultured from human PDL tissue. (**c**-**f**) Flow cytometry analysis of CD34, CD45, CD73 and CD90 in PDLCs. (**g**) Red nodules of mineralization by Alizarin Red S. Black arrows: Red nodules of mineralization. (**h**) Positive lipid accumulation by oil red O. Black arrows: Oil Red O-positive lipid accumulation. (**i**) PDLCs with chondrogenic induction solution, blue chondroid cells can be seen by Alcian blue staining. Black arrows: Blue chondroid cells. Scale bar = 100 μm

markers (CD73 and CD90) (Fig. 1e-f). These results suggest PDLCs were successfully cultured.

PDLCs were treated by different concentrations of LAP. LAP showed cytocompatibility in the range of 0–100 μg·mL^{-1} (Fig. 2b). Figure 2c and e show the ALPL staining and ALPL activity of PDLCs treated by LAP after 7 days. Dark blue staining indicated an increase in ALP activity as elevated LAP concentrations. There are more cell staining and ALP activity in 50 μg·mL^{-1} and 100 μg·mL^{-1} groups, particularly evident at 100 μg·mL^{-1}. Alizarin red S staining showed most pronounced red nodule formed in 100 μg·mL^{-1} group (Fig. 2d and f),

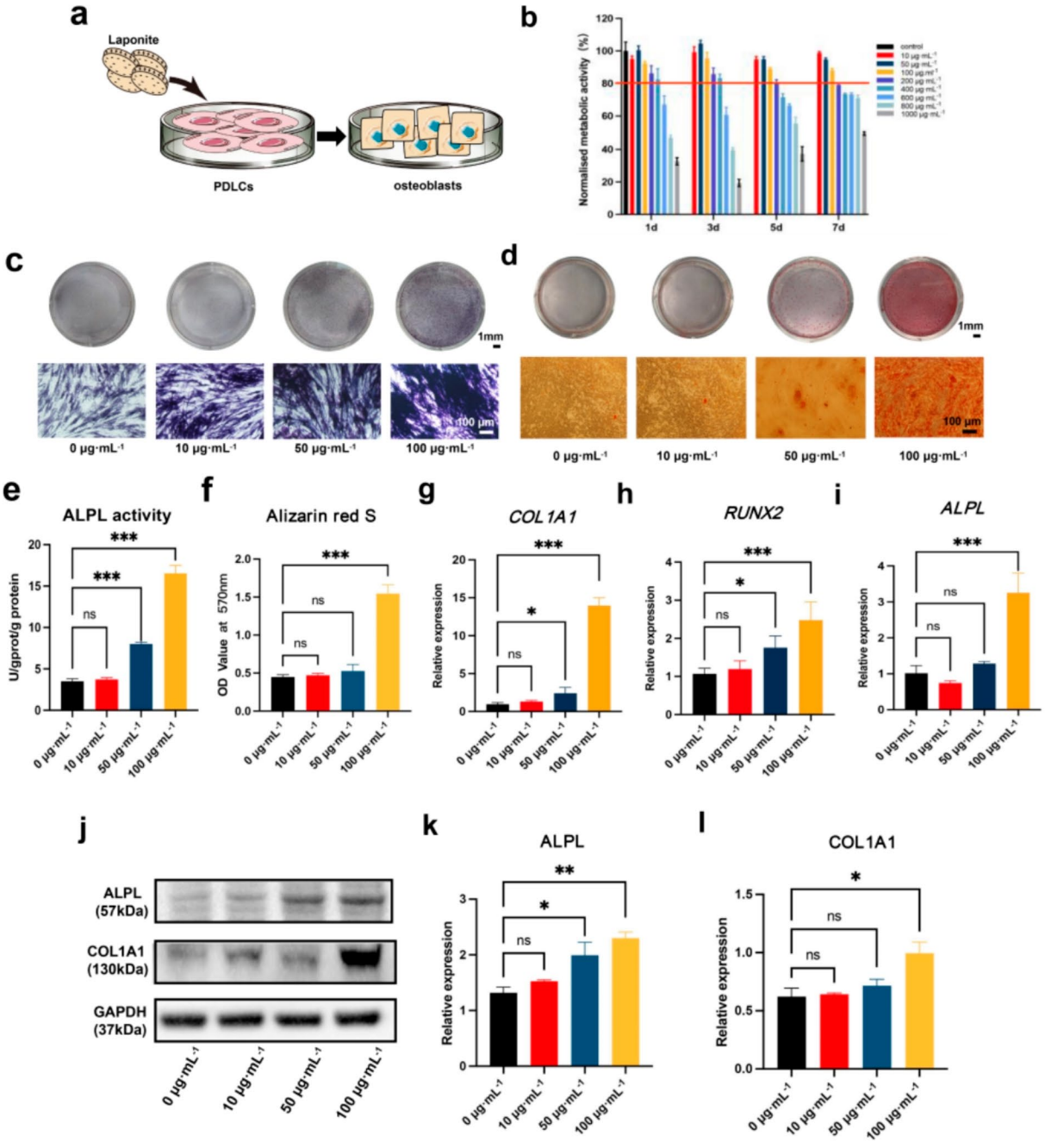

Fig. 2 LAP promoted PDLCs osteogenic differentiation. (**a**) Schematic diagram of LAP promoting osteogenic differentiation of PDLCs. (**b**) The metabolic activity of PDLCs stimulated by different concentrations of LAP. (**c**, **e**) ALPL staining and activity of PDLCs stimulated by LAP for 7 days. (**d**, **f**) Alizarin red staining and quantification of PDLCs cultured by LAP for 21 days. (**g**-**i**) qPCR results of osteogenic-related genes (*COL1A1*, *RUNX2* and *ALPL*) of PDLCs stimulated with LAP for 7 days. (j-l) Western blot analysis of osteogenic-related proteins (ALPL and COL1A1) of PDLCs stimulated with LAP for 7 days. Scale bar = 1mm and 100 μm. *$p < 0.05$; **$p < 0.01$; ***$p < 0.001$ compared with the control (LAP at 0 μg·mL^{-1})

which indicated that LAP enhanced mineralized matrix formation. The expression levels of osteogenic differentiation genes and proteins in PDLCs were estimated after treated by LAP for 7 days. LAP significantly upregulated the expression of *COL1A1*, *RUNX2* and *ALPL*, with maximum expression observed at 100 μg·mL^{-1} (Fig. 2g-i). Also, increased ALPL and COL1A1 protein levels of PDLCs could be observed in a dose-dependent manner (Fig. 2j-l). The results collectively demonstrated that LAP could promote osteogenic differentiation and mineralization of PDLCs.

LAP induced PDLCs cementogenic differentiation

To further evaluate the capacity of LAP on cementogenic differentiation of PDLCs, typical cementogenic differentiation genes (*CAP* and *CEMP1*) were selected to estimate the expression levels following PDLCs were stimulated with LAP for 7 days. As depicted in Fig. 3b and c, the relative expression levels were progressively upregulated and subsequently increased in a dose-dependent manner, with the highest expression observed at a LAP concentration of 100 μg·mL^{-1}. Accordingly, CAP and CEMP1 protein levels of PDLCs treated by LAP showed the same trend as genes expression. The maximum expression amount is 100 μg·mL^{-1} of LAP (Fig. 3d-f). These results suggested that LAP could accelerate cementogenic differentiation of PDLCs.

PDLCs stimulated by LAP indirectly enhanced angiogenesis

LAP with concentration of 100 μg·mL^{-1} was chosen for further experiments based on the above results. To further elucidate the potential effects of LAP on PDLCs-induced regeneration processes, a series experiments were carried out to evaluate whether LAP modulates angiogenesis by PDLCs in a paracrine manner. PDLCs were cultured by 0 μg·mL^{-1} and 100 μg·mL^{-1} LAP for 3 days, and the supernatants were then collected and added to HUVECs. As shown in Fig. 4b and c, cell migration was clearly observed in the LAP group compared to the control group. Moreover, more tube-like structures were observed in the LAP group, the tube length and the number of tube junctions were significantly higher than the control group (Fig. 4d-f). Furthermore, qPCR analysis was used to assess the expression levels of different

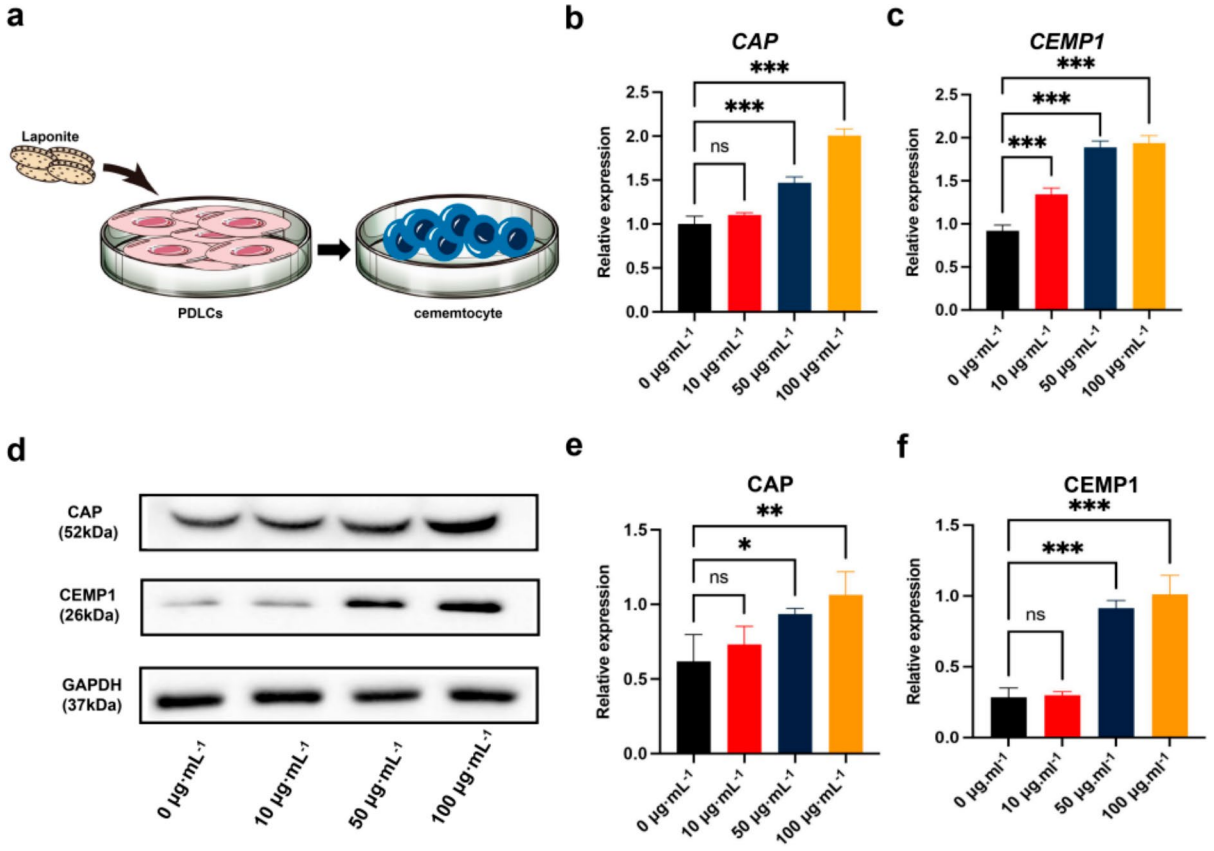

Fig. 3 LAP-induced PDLCs cementogenic differentiation. (**a**) Schematic diagram of LAP promoting cementogenic differentiation of PDLCs. (**b**, **c**) The expression levels of cementogenic differentiation genes (*CAP* and *CEMP1*) of PDLCs after 7 days of incubation with various doses of LAP. (**d**-**f**) WB analysis of cementogenic differentiation proteins (CAP and CEMP1) of PDLCs stimulated with various doses of LAP for 7 days. *$p < 0.05$; **$p < 0.01$; ***$p < 0.001$ compared with the control (LAP at 0 μg·mL^{-1})

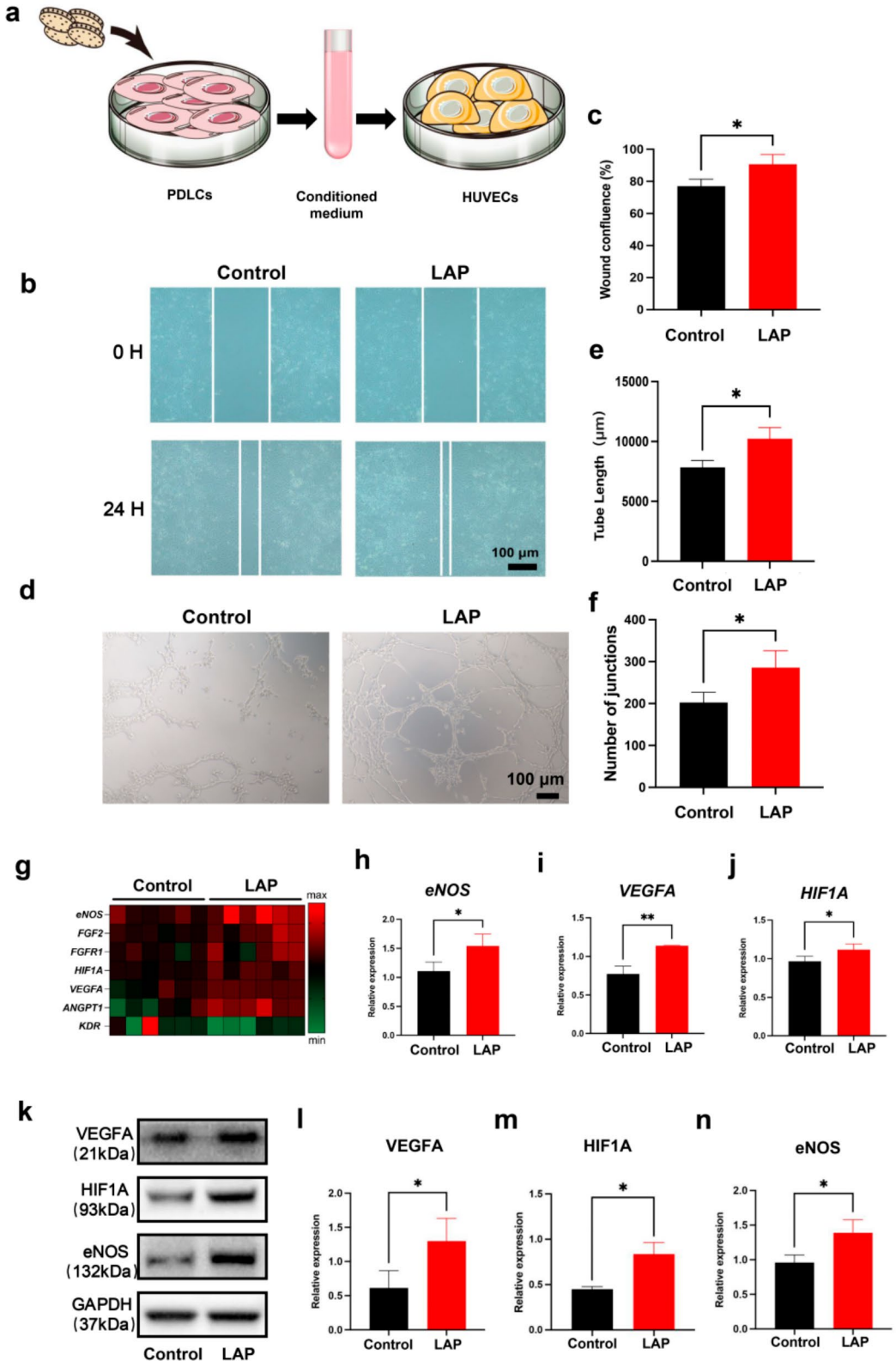

Fig. 4 PDLCs stimulated by LAP indirectly enhanced angiogenesis. (**a**) Schematic diagram of PDLCs stimulated by LAP enhanced angiogenesis of HUVECs. (**b**-**c**) Scratch wound healing assays. (**d**-**f**) Tube formation assays. (**g**). Angiogenesis-related gene expression magnitude heatmap. (**h**-**j**) mRNA expression levels of angiogenesis-related genes (*VEGFA*, *HIF1A* and *eNOS*) of HUVECs. (**k**-**n**) Western blot analysis of angiogenesis proteins (VEGFA, HIF1A, and eNOS) of HUVECs. Scale bar = 100 μm. *$p < 0.05$; **$p < 0.01$; ***$p < 0.001$ compared with the control (LAP at 0 μg·mL^{-1})

cytokines associated with angiogenesis in HUVECs. The heatmap of mRNA expression levels of angiogenesis-related gene is shown in Fig. 4g. Notably, the expression of angiogenesis-related gene and protein (HIF1A, VEGFA and eNOS) in HUVECs were significantly enhanced in the LAP group compared to control group (Fig. 4g-n). Taken together, these results showed PDLCs stimulated with LAP promoted angiogenesis of HUVECs in vitro.

The uptake of LAP by PDLCs

In order to track the pathway and extent of LAP uptake by PDLCs, confocal laser scanning microscopy was used to position rhodamine-marked LAP, which was uptook by PDLCs. Figure 5c illustrates a small amount of LAP could be observed on the cell membrane of PDLCs within 2 h. Over time, LAP cellular uptake exhibited a time dependent increase. The ingested LAP aggregated enlarging in size and number and distributed throughout the cell membrane to the nucleus. At day 7, the internalized LAP was predominantly localized around cell nucleus (Fig. 5g). It demonstrated that LAP could be easily taken up by PDLCs to further regulate cellular activity.

RNA sequencing analysis of PDLCs treated with LAP

To further explore the potential mechanism of LAP on PDLCs, RNA sequencing analysis of PDLCs treated by LAP was carried out. KEGG pathway analysis was performed to investigate the potential signaling pathways and the enriched pathways are presented in Fig. 6b. The PI3K-AKT pathway attracted our attention. GO analysis of differentially expressed genes showed that the PI3K-AKT pathway components were upregulated in the LAP group (Fig. 6c). To verify the influence of PI3K-AKT signaling pathway on PDLCs treated with LAP, the protein expression level of PI3K, P-AKT, AKT, P-mTOR and mTOR, key components of the PI3K-AKT signaling pathway, were evaluated. As shown in Fig. 6d-g, the expression of PI3K and the phosphorylation levels of AKT and mTOR in PDLCs stimulated with LAP were significantly higher than the control group, which is consistent with transcriptome sequencing results.

LAP promoted osteogenesis and cementogenesis of PDLCs *via* PI3K-AKT signaling pathway activation

To verify the effects of PI3K-AKT signaling pathway on LAP-mediated osteogenesis and osteogenic differentiation of PDLCs, LY294002 (LY), an inhibitor of PI3K, was added to the LAP group to inhibit PI3K-AKT pathway activation. The expression of key marker proteins (P-AKT, AKT, P-mTOR, mTOR and PI3K) in the PI3K-AKT signalling pathway was significantly decreased after LY treatment (Fig. 7a-d). Accordingly, the increased

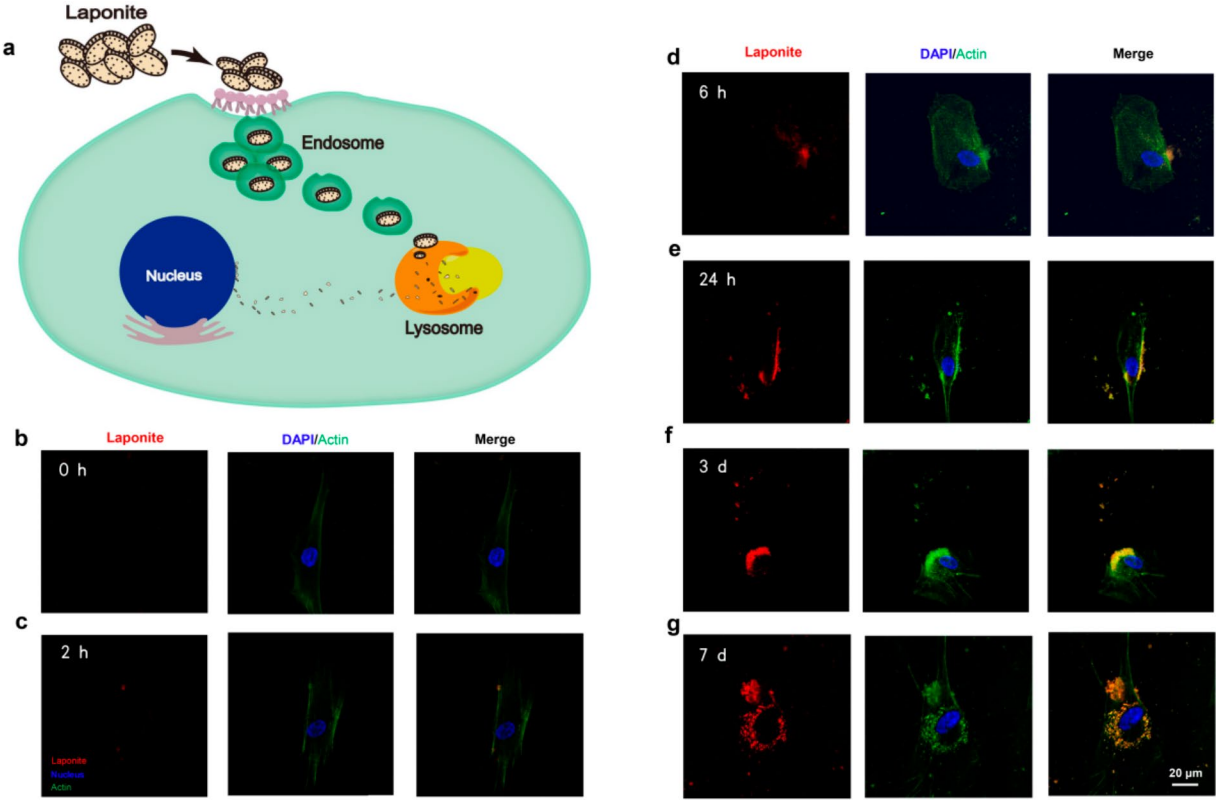

Fig. 5 The uptake of LAP by PDLCs. (**a**) Schematic diagram of cellular uptake of LAP. Cellular uptake of LAP at 0 h (**b**), 2 h (**c**), 6 h (**d**), 24 h (**e**), 3d (**f**) and 7d (**g**). Scale bar = 20 μm. Red (RB-labelled Laponite particles), blue (nucleus), green (actin). Scale bar = 20 μm

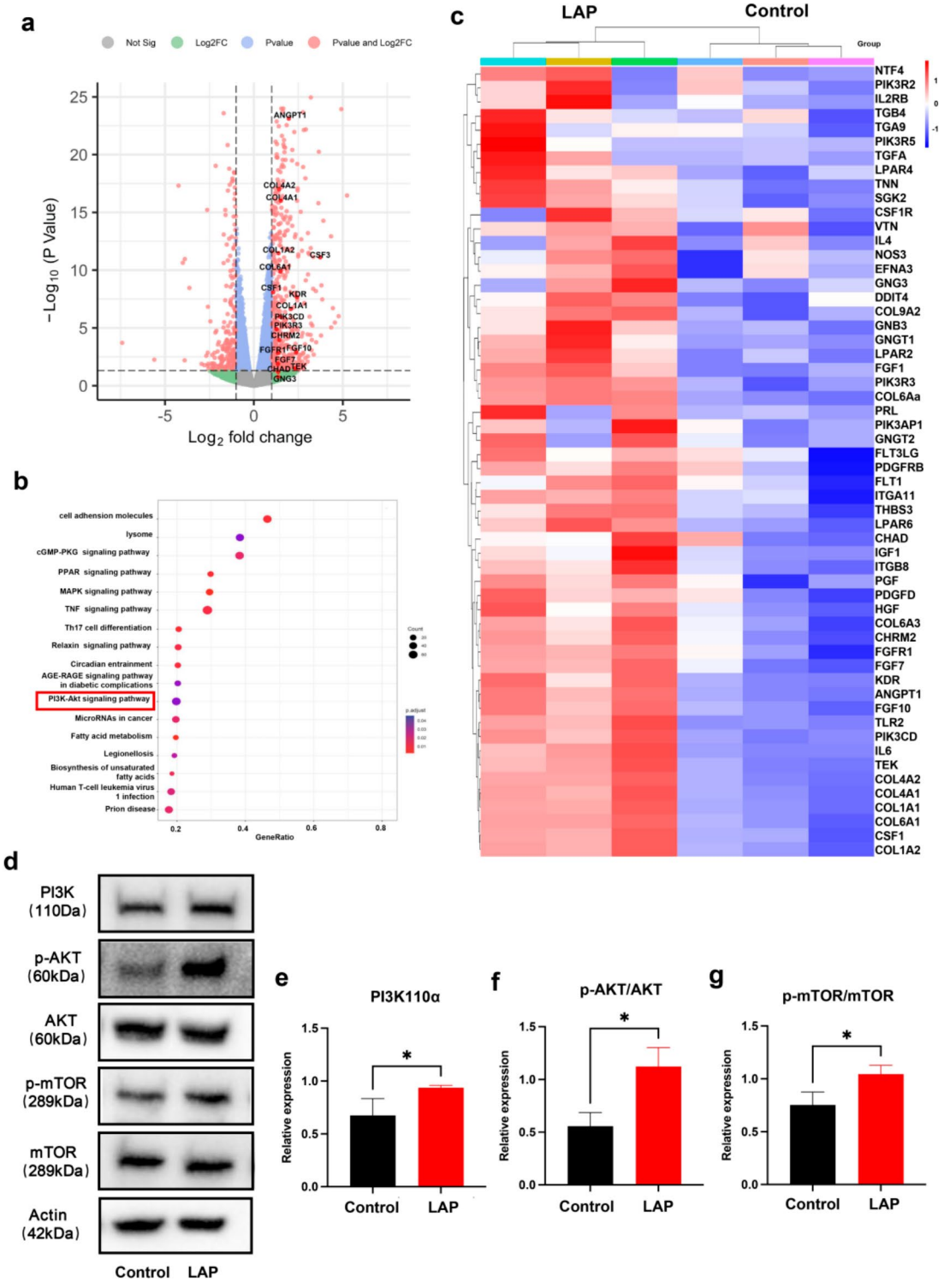

Fig. 6 RNA sequencing analysis of PDLCs treated with LAP. (**a**) Volcano plots showing mRNA expression profiles of PDLCs cultured in the two groups. (**b**) KEGG pathway gene enrichment analysis between the PDLCs treated with LAP. (**c**) The heat map showing expression levels of PI3K-AKT signaling pathways associated genes identified by GO enrichment analysis. (d-g) PI3K, AKT, P-AKT, mTOR and P-mTOR protein expression were measured by Western blot analysis. *$p < 0.05$ compared with the control (LAP at 0 μg·mL^{-1})

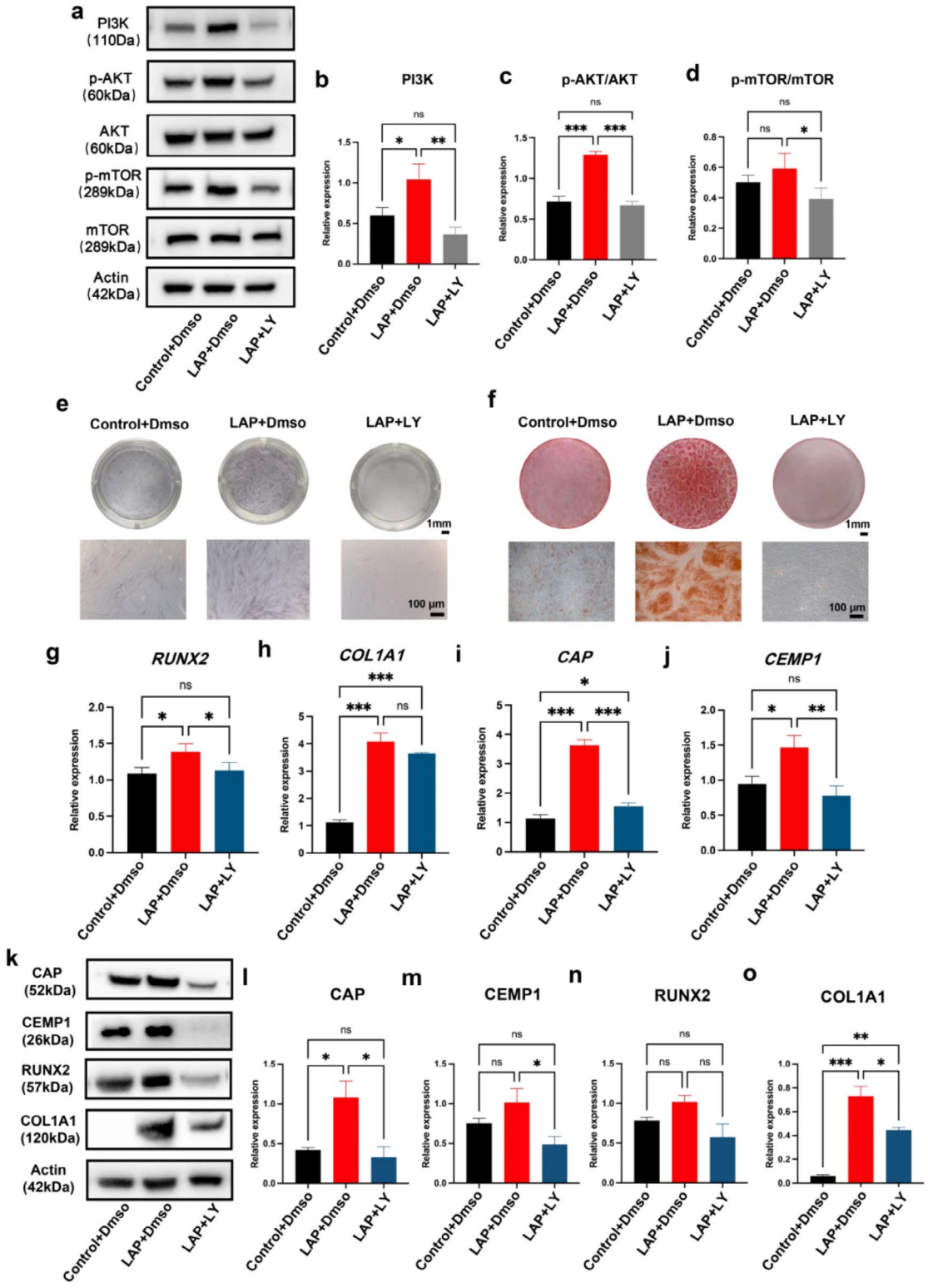

Fig. 7 LAP promoted osteogenesis and cementogenesis of PDLCs. ***via*** PI3K-AKT signaling pathway activation. (**a**-**d**) PI3K, AKT, P-AKT, mTOR, and P-mTOR protein expression were measured by western blot analysis. (**e**) ALPL staining. (**f**) Alizarin Red S staining. (**g**-**j**) The expression levels of genes associated to osteogenic and cementogenic differentiation (*RUNX2*, *COL1A1*, *CAP* and *CEMP1*). (**k**-**o**) The expression levels of proteins associated to osteogenic and cementogenic differentiation (RUNX2, COL1A1, CAP *and* CEMP1) were measured by western blot analysis. Scale bar = 1mm and 100 μm. *$p < 0.05$; **$p < 0.01$; ***$p < 0.001$

ALPL expression and mineralized nodule formation levels also suppressed in the LAP+LY group (Fig. 7e-f). The expression of osteogenic and cementogenic differentiation genes and proteins (RUNX2, COL1A1, CAP and CEMP1) were significantly decreased after LY treatment in LAP+LY group (Fig. 7g-o). The above results indicated that suppressing PI3K-AKT signaling pathway would abort LAP-induced osteogenic and cementogenic differentiation of PDLCs, which suggested LAP promoted osteogenesis and cementogenesis of PDLCs *via* PI3K-AKT signaling pathway activation.

LAP improved rat periodontal defect regeneration in vivo

As shown in Fig. 8a, more bone formation outside mandibular bone contours of periodontal defects. The bone mineral density (BMD) and volume ratios of new bone to total tissue (BV/TV) analysis showed a higher volume and density of new bone in the periodontal defect in LAP group than control group (Fig. 8b-c). Additionally, the Tb.N levels in the LAP group was higher than that in the control group (Fig. 8d). Histological staining and analysis showed only limited amount of bone formed in the control groups, and more new bone formation at the edge of rat periodontal defects in LAP group (Fig. 8e-f). Few attached fibers attached to root surface in control group. But in LAP group, more dense mature bone formed around root surface, and homogeneous collagen fibers and mature bone could also be observed on the adjacent root surfaces, indicating new attachment formation in the periodontal defect. Quantitative analysis also indicated new bone and new attachment formation rate were significantly higher in LAP group than control group (Fig. 8g-h). Additionally, CD31 was used as a marker for vessels in immunofluorescent staining to evaluate new vessel formation in periodontal defects (Fig. 8i). Quantitative analysis indicated a significantly higher area of CD31-positive cells in the LAP group compared to the control group, suggesting that LAP can accelerate blood vessel formation during the periodontal regeneration process (Fig. 8j). These results confirmed the regulatory effects of LAP on periodontal regeneration.

Discussion

Bioactive materials have been widely used in periodontal tissue regeneration, which generate special biological or chemical reactions on the surface or interface of materials [28]. These reactions can impact the interaction between tissues and materials, stimulate cell activity

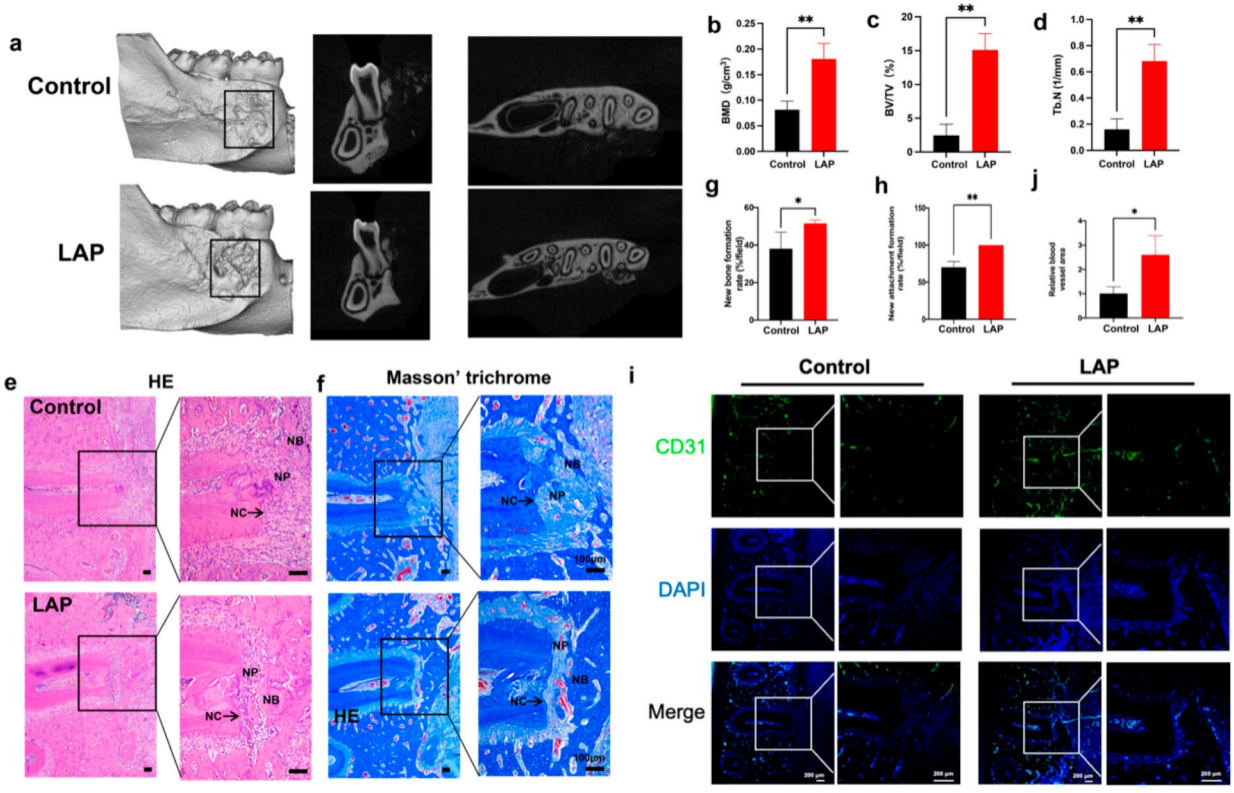

Fig. 8 LAP improved rat periodontal defect regeneration. (**a**) Representative micro-CT reconstructed images of rat periodontal defects. (**b**-**d**) BMD, BV/TV ratio and Tb.N of Micro-CT data analysis. (**e**-**f**) Histological HE and Masson's trichome-stained of rat periodontal defects. (**g**-**h**) Histological quantitative analysis of new bone formation rate and new attachment formation rate. (**i**) Immunofluorescent staining of CD31 in periodontal defects areas. (**j**) Quantitative analysis of CD31-positive cells. NC, new cementum; NP, new periodontal ligaments; NB, new bone. Scale bar = 100 and 200 μm. *$p < 0.05$; **$p < 0.01$

and induce tissue regeneration. In this study, for the first time, we found that LAP could improve osteogenic and cementogenic differentiation of PDLCs, and this regulatory effects of LAP on PDLCs differentiation were closely correlated with activation of PI3K-AKT signaling pathway. Additionally, LAP enhanced angiogenesis indirectly *via* manipulating paracrine of PDLCs. Furthermore, LAP could enhance periodontal defect regeneration in vivo. Our data refined the underlying mechanisms of LAP on periodontal regeneration and highlighting it could serve as a promising therapeutic option in periodontal therapy.

As contributors to new bone and cementum formation, PDLCs aid in the restoration of damaged tooth-supporting tissue by periodontitis [29]. To promote osteogenesis and cementogenesis of PDLCs, a variety of periodontal regeneration techniques have been used [30, 31]. Several studies have shown that nanomaterials, such as iron oxide nanoparticles, AuNPs, could promote the osteogenic differentiation of PDLCs and further promote periodontal tissue regeneration [32, 33]. Our results indicated that stimulation of PDLCs with LAP can promote the formation of ALP and mineralized nodules, along with activation of the key transcription factor (RUNX2) during osteogenic differentiation. Additionally, the downstream osteogenic related expression factors (COL1A1) was significantly increased by the addition of LAP, which showed dose dependence. These results were consistent with the conclusions of Carrowand Xavier et al., which indicated that LAP could promote human mesenchymal stem cells osteogenic differentiation [18]. Interestingly, we found that the cementum-specific proteins CAP and CEMP1 in PDLCs were also significantly upregulated after being treated with LAP. CEMP1 and CAP are known cementogenic-related proteins capable of stimulating cementogenic differentiation [34, 35]. These results represented the inaugural demonstration that two-dimensional nanomaterial LAP can enhance the cementogenic differentiation of PDLCs and might play regulatory role in cementogenesis.

Vascularization acts as a crucial role in the network of regenerative tissue formation, providing oxygen, nutrients, and growth factors to the regeneration sites [36, 37]. Given the deep link between periodontal tissue regeneration and angiogenesis, the ideal periodontal regeneration therapy must consider the vascularization regulation [38, 39]. Some biomaterials, such as hierarchical porous biomimetic sponges and extrusion-printed scaffolds, markedly enhance endogenous vascularized bone tissue regeneration by augmenting the paracrine effects of MSCs [40, 41]. HUVECs possess the typical functions of vascular endothelial cells and are widely used in angiogenesis research [42, 43]. Iwasaki et al. found that the conditioned medium from PDLCs improved the viability of HUVECs and modulated angiogenesis in a paracrine manner, presenting a promising strategy for periodontal tissue regeneration [44]. In our previously study, we also found that PCL/LAP scaffold improved angiogenesis of HUVECs through regulating the paracrine of osteoblasts [22]. The current study indicated that PDLCs treated with LAP indirectly enhanced the migration capacity of HUVECs, promoted vascularization, and significantly upregulated the expression of angiogenic genes and proteins (VEGFA, HIF1A, and eNOS). It might be attributed to the paracrine effects mediated by PDLCs following stimulation with LAP.

Due to their nanoscale size, nanomaterials have the potential to effectively interact with cell membranes and intracellular fluids *via* receptor mediated endocytosis [45]. LAP ($Na^{+0.7}[(Si_8Mg_{5.5}Li_{0.3})O_{20}(OH)_4]^{-0.7}$) belongs to artificially synthesized nanoclay, comprised of bioactive silicate nanoplatelets. It can degrade into Mg^{2+}, $Si(OH)_4$, and Li^+, which are cytocompatible and facilitate normal cellular metabolism and proliferation [18, 46, 47]. Mousa and Gahawar et al. previously found that LAP could be internalized by BMSCs in a time dependent manner and undergone degradation in lysosomes [18, 48]. To further explore the interaction between LAP and PDLCs, LAP was labeled with rhodamine red B using its non-specific adsorption property and then co-cultured with PDLCs. The results revealed that LAP could be rapidly aggregated outside the cell membrane, uptaked by PDLCs *via* endocytosis, and with prolonged exposure, gradually accumulated around the cell nucleus. Therefore, we speculated that LAP entered the PDLCs through entosis to form phagosomes, and gradually fused with lysosomes to form vesicles. With lysosomal enzymes, LAP gradually degraded into ionic products and released into the cytoplasm to promote the transformation of cells from proliferation to differentiation state, thus playing a role.

To further explore the regulatory mechanism of LAP on PDLCs, transcriptome sequencing of PDLCs was conducted. The results demonstrated a close correlation between the regulation of LAP and the PI3K-AKT signaling pathway. PI3K-AKT signaling pathway has been confirmed plays a crucial role in regulating various cellular processes, including cell growth, survival, and proliferation [49, 50]. It also found to be intimately involved in orchestrating osteogenic differentiation [51–53]. Zhu et al. developed a nanozyme to regulate osteogenic differentiation through activating PI3K-AKT pathway and ultimately promote periodontal regeneration [54].In the current study, the expression of P-AKT, P-mTOR, and PI3K in the PI3K-AKT signaling pathway was significantly increased when PDLCs stimulated with LAP. These key marker proteins were significantly decreased when the LY294002, an inhibitor of PI3K, was added to PDLCs co-cultured with LAP. Accordingly, the osteogenic and cementogenic differentiation of PDLCs stimulated with

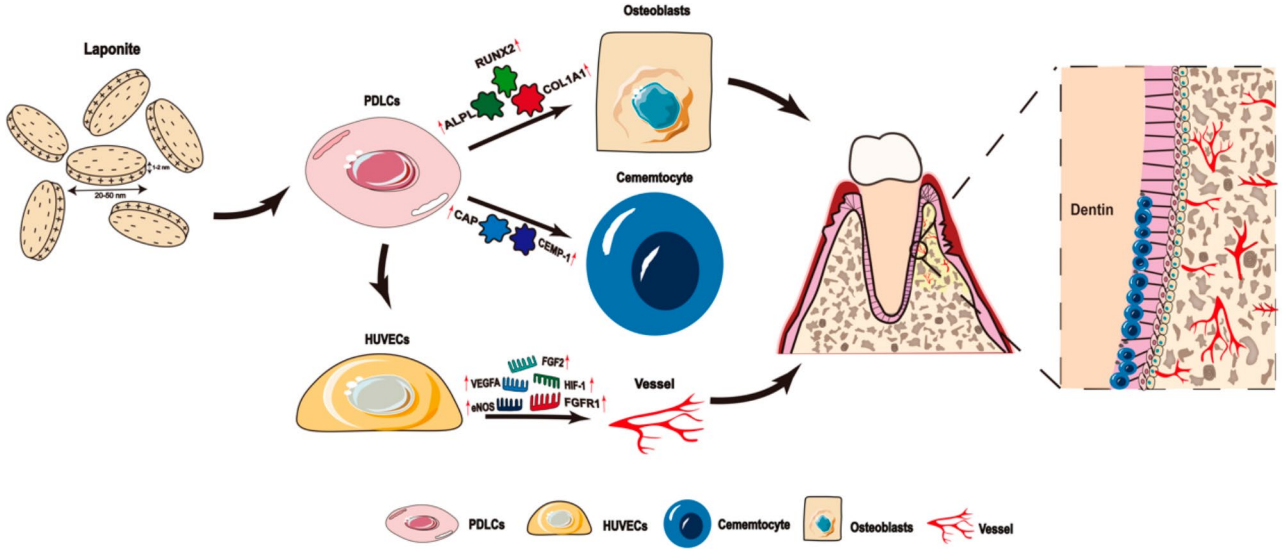

Fig. 9 Schematic illustration of the role of LAP on PDLCs for periodontal regeneration

LAP were counteracted by inhibiting the PI3K-AKT signaling pathway. These data demonstrated that LAP degradation may occur subsequent to endocytosis, with the resultant ionic products activating the PI3K-AKT signaling pathway in PDLCs, leading to cementogenesis as well as osteogenesis. This activation subsequently promotes the transcription of RUNX2, COL1A1, CAP and CEMP1, initiating new bone and cementum formation, ultimately facilitating periodontal regeneration. As far as we know, this is the first study to reveal that LAP promoted cell differentiation *via* PI3K-AKT signaling pathway activation. However, the exact mechanisms involved still need to be further explored.

The goal of periodontal therapy is to achieve periodontal regeneration. Currently, rat mandibular periodontal defect model has been widely used to explore the effectiveness of distinct regenerative approaches [55]. It provides a stable local environment for bone, periodontal ligament and cementum regeneration. In the present study, LAP was implanted into rat mandibular periodontal defects. The results demonstrated that LAP enhanced more vascular bone formation during periodontal regeneration. Furthermore, the formation of new attachments was markedly enhanced. We speculated that the released LAP might mobilize PDLCs within periodontal defect sites, directly enhancing osteogenic and cementogenic differentiation, ultimately leading to the formation of new alveolar bone and cementum. Furthermore, LAP may indirectly modulate the paracrine of PDLCs, thereby promoting vascularization to facilitate periodontal tissue regeneration.

Periodontal tissue regeneration involves a complex interplay of multiple cells and biological processes, including an early macrophage or neutrophil mediated inflammatory response, antibacterial defense, and multi-tissue regeneration of the periodontium [56–58]. Although the current study found that LAP promoted periodontal regeneration, only the effect on PDLCs were evaluated, thus limiting the elucidation of the intricate process of periodontal regeneration. Moreover, the mechanisms by which LAP binds to cells for exocytosis remain unclear, as do the precise degradation processes upon cellular entry and the specific regulatory effects on the PI3K-AKT signaling pathway, and the immune effect between LAP and immune cells is also uncertain. These uncertainties need to be further explored to offer new insights into the impact of LAP in periodontal treatment. This encompasses utilizing LAP-functionalized biomaterials for clinical applications and leveraging LAP as a drug carrier, in combination with antibiotics, growth factors, or peptide factors, to enhance its efficacy in periodontal regeneration.

Conclusion

In general, the current study indicated that LAP facilitated osteogenic and cementogenic differentiation of PDLCs *via* PI3K-AKT signaling pathway. Furthermore, LAP indirectly boosted angiogenesis by modulating the paracrine activity of PDLCs. Also, rat periodontal defect treated with LAP exhibited more periodontal tissue regeneration. To our current knowledge, this study represents the first comprehensive investigation that LAP could regulate PDLCs by activating PI3K-AKT signaling pathway and has the ability to promote periodontal defect regeneration in vivo (Fig. 9). Our results hold that LAP presents a promising candidate for periodontal therapy.

Supplementary Information

The online version contains supplementary material available at https://doi.org/10.1186/s12951-024-02798-6.

Supplementary Table 1. Primer sequences used in quantitative real-time PCR

Acknowledgements
The authors thank for the support from the Joint Funds for the Innovation of Science and Technology, Fujian Province (2020Y9032), Fujian provincial health technology project (2022QNA072), the Educational Research Project for Young and Middle-aged Teachers of Fujian Provincial Department of Education (JAT220078) and Startup Fund for scientific research, Fujian Medical University (2022QH1140).

Author contributions
ZC was involved in sample preparation, experiment conducting and data analysis and wrote the manuscript. NX and LL prepared the samples and cell experiments. LZ, FY and WH collected, analyzed and interpreted the data. ZW and YC conceived and designed the experimentst. KL and XX designed and supervised the research and revised the manuscript. All authors read and approved the final manuscript.

Funding
This study was supported by the Joint Funds for the Innovation of Science and Technology, Fujian Province (2020Y9032), Fujian provincial health technology project (2022QNA072), the Educational Research Project for Young and Middle-aged Teachers of Fujian Provincial Department of Education (JAT220078) and Startup Fund for scientific research, Fujian Medical University (2022QH1140).

Data availability
No datasets were generated or analysed during the current study.

Declarations

Ethics approval and consent to participate
All experiments were approved by the Ethics of the School and Hospital of Stomatology, Fujian Medical University (2021 Ethics Review No. 104). All animal experiments were approved by the Animal Care and Use Committee of Fujian Medical University (IACUC FJMU 2023-0036).

Consent for publication
All the authors agree to publish this study in the Journal of Nanobiotechnology.

Competing interests
The authors declare no competing interests.

Received: 10 June 2024 / Accepted: 22 August 2024
Published online: 03 September 2024

References

1. Slots J. Periodontitis: facts, fallacies and the future. Periodontol 2000. 2017;75:7–23.
2. Papapanou PN, Sanz M, Buduneli N, Dietrich T, Feres M, Fine DH, Flemmig TF, Garcia R, Giannobile WV, Graziani F, et al. Periodontitis: Consensus report of workgroup 2 of the 2017 World workshop on the classification of Periodontal and Peri-implant diseases and conditions. J Clin Periodontol. 2018;45(Suppl 20):S162–70.
3. Sculean A, Chapple IL, Giannobile WV. Wound models for periodontal and bone regeneration: the role of biologic research. Periodontol 2000. 2015;68:7–20.
4. Venkataiah VS, Handa K, Njuguna MM, Hasegawa T, Maruyama K, Nemoto E, Yamada S, Sugawara S, Lu L, Takedachi M, et al. Periodontal regeneration by allogeneic transplantation of adipose tissue derived Multi-lineage Progenitor Stem cells in vivo. Sci Rep. 2019;9:921.
5. Sallum EA, Ribeiro FV, Ruiz KS, Sallum AW. Experimental and clinical studies on regenerative periodontal therapy. Periodontol 2000. 2019;79:22–55.
6. Villar CC, Cochran DL. Regeneration of periodontal tissues: guided tissue regeneration. Dent Clin North Am. 2010;54:73–92.
7. Kao RT, Nares S, Reynolds MA. Periodontal regeneration - intrabony defects: a systematic review from the AAP Regeneration Workshop. J Periodontol. 2015;86:S77–104.
8. Lin Z, Rios HF, Cochran DL. Emerging regenerative approaches for periodontal reconstruction: a systematic review from the AAP Regeneration Workshop. J Periodontol. 2015;86:S134–152.
9. Majzoub J, Barootchi S, Tavelli L, Wang CW, Chan HL, Wang HL. Guided tissue regeneration combined with bone allograft in infrabony defects: clinical outcomes and assessment of prognostic factors. J Periodontol. 2020;91:746–55.
10. Lyons JG, Plantz MA, Hsu WK, Hsu EL, Minardi S. Nanostructured Biomaterials for Bone Regeneration. Front Bioeng Biotechnol. 2020;8:922.
11. Mostafavi E, Medina-Cruz D, Kalantari K, Taymoori A, Soltantabar P, Webster TJ. Electroconductive Nanobiomaterials for tissue Engineering and Regenerative Medicine. Bioelectricity. 2020;2:120–49.
12. Park J, Park S, Kim JE, Jang KJ, Seonwoo H, Chung JH. Enhanced osteogenic differentiation of Periodontal ligament stem cells using a graphene oxide-coated poly(ε-caprolactone) Scaffold. Polym (Basel) 2021, 13.
13. Cui D, Kong N, Ding L, Guo Y, Yang W, Yan F. Ultrathin 2D Titanium Carbide MXene (Ti(3) C(2) T(x)) nanoflakes activate WNT/HIF-1α-Mediated metabolism reprogramming for Periodontal Regeneration. Adv Healthc Mater. 2021;10:e2101215.
14. Tomás H, Alves CS, Rodrigues J. Laponite®: A key nanoplatform for biomedical applications? Nanomedicine 2018, 14:2407–20.
15. Gaharwar AK, Cross LM, Peak CW, Gold K, Carrow JK, Brokesh A, Singh KA. 2D nanoclay for Biomedical Applications: Regenerative Medicine, therapeutic delivery, and Additive Manufacturing. Adv Mater. 2019;31:e1900332.
16. Jiang T, Chen G, Shi X, Guo R. Hyaluronic Acid-Decorated Laponite(®) Nanocomposites for Targeted Anticancer Drug Delivery. Polym (Basel) 2019, 11.
17. Mihaila SM, Gaharwar AK, Reis RL, Khademhosseini A, Marques AP, Gomes ME. The osteogenic differentiation of SSEA-4 sub-population of human adipose derived stem cells using silicate nanoplatelets. Biomaterials. 2014;35:9087–99.
18. Carrow JK, Cross LM, Reese RW, Jaiswal MK, Gregory CA, Kaunas R, Singh I, Gaharwar AK. Widespread changes in transcriptome profile of human mesenchymal stem cells induced by two-dimensional nanosilicates. Proc Natl Acad Sci U S A. 2018;115:E3905–13.
19. Veernala I, Giri J, Pradhan A, Polley P, Singh R, Yadava SK. Effect of Fluoride Doping in Laponite Nanoplatelets on osteogenic differentiation of Human Dental follicle stem cells (hDFSCs). Sci Rep. 2019;9:915.
20. Li T, Liu ZL, Xiao M, Yang ZZ, Peng MZ, Li CD, Zhou XJ, Wang JW. Impact of bone marrow mesenchymal stem cell immunomodulation on the osteogenic effects of laponite. Stem Cell Res Ther. 2018;9:100.
21. Xu X, Xiao L, Xu Y, Zhuo J, Yang X, Li L, Xiao N, Tao J, Zhong Q, Li Y, et al. Vascularized bone regeneration accelerated by 3D-printed nanosilicate-functionalized polycaprolactone scaffold. Regen Biomater. 2021;8:rbab061.
22. Xu X, Zhuo J, Xiao L, Xu Y, Yang X, Li Y, Du Z, Luo K. Nanosilicate-Functionalized Polycaprolactone orchestrates Osteogenesis and osteoblast-Induced multicellular interactions for potential endogenous vascularized bone regeneration. Macromol Biosci. 2022;22:e2100265.
23. Li J, Zhang F, Zhang N, Geng X, Meng C, Wang X, Yang Y. Osteogenic capacity and cytotherapeutic potential of periodontal ligament cells for periodontal regeneration in vitro and in vivo. PeerJ. 2019;7:e6589.
24. D'Errico JA, Ouyang H, Berry JE, MacNeil RL, Strayhorn C, Imperiale MJ, Harris NL, Goldberg H, Somerman MJ. Immortalized cementoblasts and periodontal ligament cells in culture. Bone. 1999;25:39–47.
25. Iwayama T, Iwashita M, Miyashita K, Sakashita H, Matsumoto S, Tomita K, Bhongsatiern P, Kitayama T, Ikegami K, Shimbo T et al. Plap-1 lineage tracing and single-cell transcriptomics reveal cellular dynamics in the periodontal ligament. Development 2022, 149.
26. Tour G, Wendel M, Moll G, Tcacencu I. Bone repair using periodontal ligament progenitor cell-seeded constructs. J Dent Res. 2012;91:789–94.
27. Zheng B, Jiang J, Chen Y, Lin M, Du Z, Xiao Y, Luo K, Yan F. Leptin overexpression in bone marrow stromal cells promotes Periodontal Regeneration in a rat model of osteoporosis. J Periodontol. 2017;88:808–18.
28. Han X, Alu A, Liu H, Shi Y, Wei X, Cai L, Wei Y. Biomaterial-assisted biotherapy: a brief review of biomaterials used in drug delivery, vaccine development, gene therapy, and stem cell therapy. Bioact Mater. 2022;17:29–48.

29. Isaka J, Ohazama A, Kobayashi M, Nagashima C, Takiguchi T, Kawasaki H, Tachikawa T, Hasegawa K. Participation of periodontal ligament cells with regeneration of alveolar bone. J Periodontol. 2001;72:314–23.
30. Cui D, Chen C, Luo B, Yan F. Inhibiting PHD2 in human periodontal ligament cells via lentiviral vector-mediated RNA interference facilitates cell osteogenic differentiation and periodontal repair. J Leukoc Biol. 2021;110:449–59.
31. Suo L, Wu H, Wang P, Xue Z, Gao J, Shen J. The improvement of periodontal tissue regeneration using a 3D-printed carbon nanotube/chitosan/sodium alginate composite scaffold. J Biomed Mater Res B Appl Biomater. 2023;111:73–84.
32. Li L, Zhang Y, Wang M, Zhou J, Zhang Q, Yang W, Li Y, Yan F. Gold nanoparticles combined human β-Defensin 3 Gene-Modified Human Periodontal ligament cells alleviate Periodontal Destruction via the p38 MAPK pathway. Front Bioeng Biotechnol. 2021;9:631191.
33. Shi Z, Jia L, Zhang Q, Sun L, Wang X, Qin X, Xia Y. An altered oral microbiota induced by injections of superparamagnetic iron oxide nanoparticle-labeled periodontal ligament stem cells helps periodontal bone regeneration in rats. Bioeng Transl Med. 2023;8:e10466.
34. Chen X, Liu Y, Miao L, Wang Y, Ren S, Yang X, Hu Y, Sun W. Controlled release of recombinant human cementum protein 1 from electrospun multiphasic scaffold for cementum regeneration. Int J Nanomed. 2016;11:3145–58.
35. Arzate H, Zeichner-David M, Mercado-Celis G. Cementum proteins: role in cementogenesis, biomineralization, periodontium formation and regeneration. Periodontol 2000. 2015;67:211–33.
36. Liu J, Yang L, Liu K, Gao F. Hydrogel scaffolds in bone regeneration: their promising roles in angiogenesis. Front Pharmacol. 2023;14:1050954.
37. Demcisakova Z, Luptakova L, Tirpakova Z, Kvasilova A, Medvecky L, De Spiegelaere W, Petrovova E. Evaluation of Angiogenesis in an Acellular Porous Biomaterial based on Polyhydroxybutyrate and Chitosan using the Chicken Ex Ovo Chorioallantoic membrane model. Cancers (Basel) 2022, 14.
38. Pizzicannella J, Gugliandolo A, Orsini T, Fontana A, Ventrella A, Mazzon E, Bramanti P, Diomede F, Trubiani O. Engineered Extracellular vesicles from Human Periodontal-Ligament stem cells increase VEGF/VEGFR2 expression during bone regeneration. Front Physiol. 2019;10:512.
39. Shang L, Liu Z, Ma B, Shao J, Wang B, Ma C, Ge S. Dimethyloxallyl glycine/nanosilicates-loaded osteogenic/angiogenic difunctional fibrous structure for functional periodontal tissue regeneration. Bioact Mater. 2021;6:1175–88.
40. Lian M, Sun B, Han Y, Yu B, Xin W, Xu R, Ni B, Jiang W, Hao Y, Zhang X, et al. A low-temperature-printed hierarchical porous sponge-like scaffold that promotes cell-material interaction and modulates paracrine activity of MSCs for vascularized bone regeneration. Biomaterials. 2021;274:120841.
41. Qazi TH, Tytgat L, Dubruel P, Duda GN, Van Vlierberghe S, Geissler S. Extrusion printed scaffolds with varying pore size as modulators of MSC Angiogenic Paracrine effects. ACS Biomater Sci Eng. 2019;5:5348–58.
42. Yang J, Hao X, Li Q, Akpanyung M, Nejjari A, Neve AL, Ren X, Guo J, Feng Y, Shi C, Zhang W. CAGW peptide- and PEG-Modified gene carrier for selective Gene Delivery and Promotion of angiogenesis in HUVECs in vivo. ACS Appl Mater Interfaces. 2017;9:4485–97.
43. Liu Q, Zhang H, An Y, Zhang Y, He Q, Liu K, Xia Q, Zhou H. Xinkeshu tablets promote angiogenesis in zebrafish embryos and human umbilical vein endothelial cells through multiple signaling pathways. J Ethnopharmacol. 2023;314:116636.
44. Iwasaki K, Akazawa K, Nagata M, Komaki M, Peng Y, Umeda M, Watabe T, Morita I. Angiogenic effects of secreted factors from Periodontal Ligament Stem cells. Dent J (Basel) 2021, 9.
45. Nanda SS, Yi DK. Recent advances in synergistic effect of nanoparticles and its Biomedical Application. Int J Mol Sci 2024, 25.
46. Brokesh AM, Cross LM, Kersey AL, Murali A, Richter C, Gregory CA, Singh I, Gaharwar AK. Dissociation of nanosilicates induces downstream endochondral differentiation gene expression program. Sci Adv. 2022;8:eabl9404.
47. Mousa M, Evans ND, Oreffo ROC, Dawson JI. Clay nanoparticles for regenerative medicine and biomaterial design: a review of clay bioactivity. Biomaterials. 2018;159:204–14.
48. Mousa M, Kim YH, Evans ND, Oreffo ROC, Dawson JI. Tracking cellular uptake, intracellular trafficking and fate of nanoclay particles in human bone marrow stromal cells. Nanoscale. 2023;15:18457–72.
49. Ersahin T, Tuncbag N, Cetin-Atalay R. The PI3K/AKT/mTOR interactive pathway. Mol Biosyst. 2015;11:1946–54.
50. Pompura SL, Dominguez-Villar M. The PI3K/AKT signaling pathway in regulatory T-cell development, stability, and function. J Leukoc Biol 2018.
51. Liu X, Chen M, Luo J, Zhao H, Zhou X, Gu Q, Yang H, Zhu X, Cui W, Shi Q. Immunopolarization-regulated 3D printed-electrospun fibrous scaffolds for bone regeneration. Biomaterials. 2021;276:121037.
52. Gao S, Chen B, Zhu Z, Du C, Zou J, Yang Y, Huang W, Liao J. PI3K-Akt signaling regulates BMP2-induced osteogenic differentiation of mesenchymal stem cells (MSCs): a transcriptomic landscape analysis. Stem Cell Res. 2023;66:103010.
53. Chen J, Liu Z, Zhang H, Yang Y, Zeng H, Zhong R, Lai S, Liao H. YBX1 promotes MSC osteogenic differentiation by activating the PI3K/AKT pathway. Curr Stem Cell Res Ther. 2023;18:513–21.
54. Zhu B, Wu J, Li T, Liu S, Guo J, Yu Y, Qiu X, Zhao Y, Peng H, Zhang J, et al. A glutathione peroxidase-mimicking Nanozyme precisely alleviates reactive oxygen species and promotes Periodontal Bone Regeneration. Adv Healthc Mater. 2024;13:e2302485.
55. Padial-Molina M, Rodriguez JC, Volk SL, Rios HF. Standardized in vivo model for studying novel regenerative approaches for multitissue bone-ligament interfaces. Nat Protoc. 2015;10:1038–49.
56. Xu T, Xie K, Wang C, Ivanovski S, Zhou Y. Immunomodulatory nanotherapeutic approaches for periodontal tissue regeneration. Nanoscale. 2023;15:5992–6008.
57. Wang S, Wang P, Thompson R, Ostrikov K, Xiao Y, Zhou Y. Plasma-activated medium triggers immunomodulation and autophagic activity for periodontal regeneration. Bioeng Transl Med. 2023;8:e10528.
58. Polimeni G, Xiropaidis AV, Wikesjö UM. Biology and principles of periodontal wound healing/regeneration. Periodontol 2000. 2006;41:30–47.

Publisher's note